Sygnatura: © Pol J Radiol, 2008; 73(2): 65-76

Polish Journal of Radiology
www.PolRadiol.com
REVIEW ARTICLE

Otrzymano: 2007.08.01
Zaakceptowano: 2007.11.26

Diagnostic imaging of primary malignant bone tumors in children (osteosarcoma, Ewing`s sarcoma) – part II

Kamil Wermeński[1], Hanna Brągoszewska[1], Anna Romaniuk-Doroszewska[1], Izabela Kopyś-Wiszniewska[1], Maria Uliasz[1], Beata Iwanowska[1], Monika Bekiesińska-Figatowska[1], Małgorzata Jastrzębska[1], Wojciech Woźniak[2]

[1] Department of Diagnostic Imaging, Institute of Mother and Child, Poland
[2] Department of Pediatric and Juvenile Tumor Surgery, Institute of Mother and Child, Poland

Author's address: Hanna Brągoszewska, Department of Diagnostic Imaging, Institute of Mother and Child, ul. Kasprzaka 17a, 01-211 Warszawa, e-mail: zakład.rtg@imid. med.pl

Summary

Neoplastic conditions of developmental period are an important problem in oncology and pediatrics. Multi-agent chemotherapy introduced in the 1970's of the last century significantly improved the results of treatment but still these tumors are the 2nd cause of death in children and adolescents.

Primary malignant bone tumors account for 1-1.5% of all neoplasms and for 7% of developmental period tumors. Depending on the kind of tissue, bone tumors demonstrate various patterns of growth, infiltration and internal architecture. Imaging methods are an important part of diagnostics and the most effective tool of monitoring response to treatment.

Plains films were the only imaging technique for many years. In the 2nd half of 20th century, angiography was introduced. Despite invasiveness, it showed malignant character of the tumor and its extension in soft tissues.

In the 7th decade of the last century, ultrasound and computed tomography started being routinely used in clinical practice. After a few years, resolution of these modalities was improved so that they could better visualize musculoskeletal tumors.

Magnetic resonance imaging was the next step, this method came into use in Poland 16 years ago. MRI is the best modality to show the extent of marrow involvement,

All the imaging techniques have their place in the diagnostic algorithm of bone tumors. Scintigraphy plays an important role in detecting skeletal metastases and disseminated disease. Fusion of radiological and nuclear medicine methods, PET-CT, brings new possibilities to musculoskeletal tumor diagnostics.

Key words: **Bone tumors • osteosarcoma • Ewing`s sarcoma • diagnostics • radiographs • ultrasound • computed tomography • magnetic resonance imaging**

PDF file: http://www.polradiol.com/fulltxt.php?ICID=857109

COMPUTED TOMOGRAPHY (CT)

The third imaging technique that should be used besides conventional radiography and ultrasonography in bone tumor diagnostic procedures in order to determine the character of the tumor and the extent of the neoplastic process is magnetic resonance (MRI) or computed tomography (CT). MRI is the best for assessment of the soft tissues and marrow cavity, as well as the neurovascular bundles [25]. MRI visualizes also bone lesions, but many authors still regard CT as the best method for assessment of the cortical layer of the bone, periosteal reactions, as well as calcifications and ossifications present in the tumor of the soft tissue [5, 6, 13, 23, 25]. Additionally, CT is considerably

cheaper and more available, and, if performed correctly, provides a lot of useful information. The limitation of this method is exposure of the patient to ionizing radiation and iodine-based contrast media.
CT is routinely used as the most important method in search for pulmonary metastases [1, 5, 13, 23, 24, 25].

Apparatus

The physical phenomenon utilized in CT is, like in conventional radiography, attenuation of X radiation by the object present on its route. The intensity of X radiation after passing through the examined object is measured in a detector placed on the other side. Many thousand such measurements are performed during such a process and after data processing an image of a single layer perpendicular to the long axis of the body is obtained. The measurements of X rays passing through the body provide the basis for reconstruction of radiation attenuation coefficients for the tissues located in the examined plane. The value of the attenuation coefficient is a composite function of X radiation energy quantum and atomic numbers of elements and electron density of the tissues. Various atomic numbers of elements and their variable content in the tissues allow to obtain images in various shades of gray, dependent on radiation attenuation coefficients, assessed in Hounsfield units. Osseous tissue containing high amounts of calcium has attenuation coefficients of 1000 and more Hounsfield units. By appropriate selection of the window level and width, various scales of values allowing to assess soft tissues and bones in the same layer can be obtained [13, 33]. High resolution and possibility of computed data processing allows precise assessment of the structure of examined organs and visualization of pathologic foci even 1 mm in diameter. The contrast of CT images can be increased by administration of a contrast medium.

The CT scanners used today belong to the third and fourth generations. The number of detectors, arranged in a few rows, reaches several hundred, and a fan-like X-ray beam covers the whole object during one impulse, with simultaneous shift of the patient at a constant rate (helical CT) [34]. This markedly reduces the examination time and increases the reconstruction potential of the technique (3D reconstruction). Bone tumors can be examined also with a single-row CT scanner, but the potential for reconstruction for surgical purposes will be worse. Tissue blood supply studies, investigating perfusion of neoplastic tissue, requiring special software for dynamic perfusion imaging, will be increasingly important in modern diagnostics.

Lungs should be examined with helical CT scanners only, because of their characteristics: short examination time makes it possible to perform the scan during one inspiration, which eliminates the effect of „omitted" and „overlapping" layers present in classic sequential CT [24].

The examinations can be documented as photos, but more and more frequently the images are stored in electronic form, especially useful for presentation of 3D reconstructions.

Methodology of CT imaging

CT in musculoskeletal system tumors is first performed for diagnostic purposes, the second time after induction chemotherapy as a preoperative examination, alone or supplementary to MRI [1]. In the postoperative period it is performed as a control examination after radical and conservative surgery with placement of bone implants. CT assessment after conservative surgery using endoprostheses or other large metal elements is more difficult because of artifacts. Conventional radiography and sonography are predestined for postoperative control of bone tumors. In the therapeutic period, CT is performed rarely, for special indication, e.g. for confirmation of tumor progression or lack of response to the applied treatment. It can also be used for monitoring of chemo- or radiotherapy in case of inoperable tumors, as it visualizes changes in the bone taking place as a result of the therapy, differences in the size and structure of soft tissue tumors, changes of blood flow in the tumor, bone marrow remodeling and periosteal reactions [5, 6, 25].

CT for bone tumor diagnostics must meet specific requirements: high-resolution software (tissue contrast resolution – 0.2 %, linear resolution below 1 mm), matrix 512x512, an appropriate window and filter for bones and soft tissue.

Window values are dependent on the quality of a specific CT scanner and camera, they should be adjusted individually, also to the assessed structure (e.g. cortical layer or periosteal reaction). The most frequently used approximate values are: bone window W = 1000-3000 HU, L = 200-600 HU, soft tissue window W = 300-500 HU, L = 30-60 HU.

Slice thickness and table shift rate depend on tumor size determined on the basis of conventional radiography. For tumors with the longitudinal dimensions not exceeding 5 cm, slice thickness and table shift ranges from 2 to 5 mm. In case of larger tumors, slice thickness is 5-10 mm, whereas table shift rate reaches 10 mm. For more detailed imaging of a selected fragment of the tumor, slice thickness and table shift can be reduced to 1-2 mm [35].

The scan should cover the joint proximal to the bone lesion down to the level of normal bone marrow density values, always beyond the extent of the tumor. If the tumor is large, both joints should be included within the scanned area. It is also advisable for the purposes of potential conservative surgery, that the tomogram should visualize the examined bone with both joints, which will allow accurate measurements of the extremity.

If possible, comparative examination of the extremities is performed, always in case of legs and forearms. It is rarely possible for the humerus.

Non-ionic contrast medium is administered intravenously in the amount of 1 ml/kg, in case of large soft tissue tumors 1.2-1.3 ml/kg to visualize the size and morphology of these tumors as well as the vasculature and its relation to the tumor.

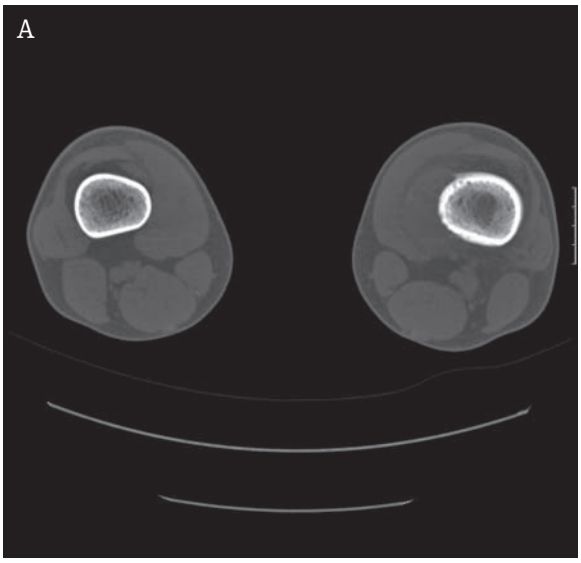

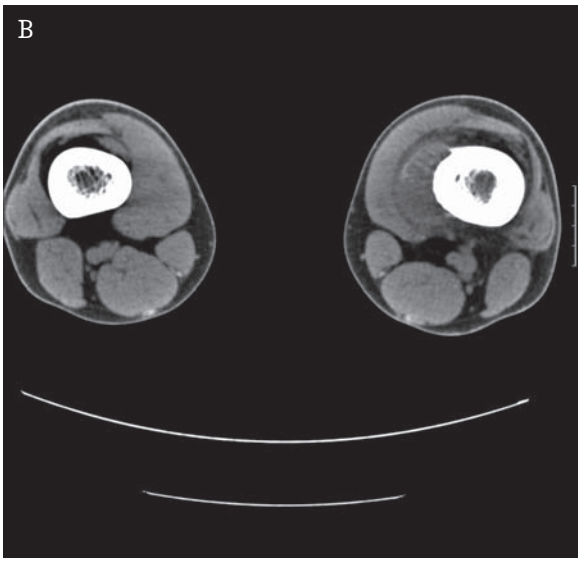

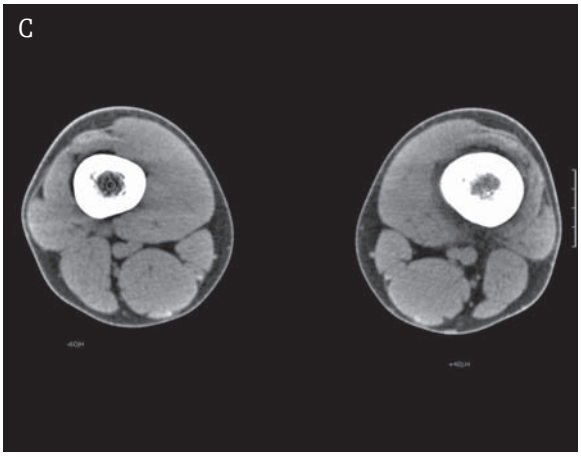

Figure 1. Osteogenic sa of the femur, CT. Patchy lytic changes, periosteal elevation, Codman's triangle, discretely calcified spicular reactions. Poorly demarcated inhomogenous extracortical tumor, with hypodense foci and tiny calcifications. **A**. Bone window. **B**. Soft tissue window. **C**. Infiltration of the medullary cavity.

Diagnostic period

During the diagnostic period, CT is performed to assess the character and stage of the tumor, i.e.

1) localization
2) size
3) character of bone lesions
4) periosteal reaction
5) involvement of the marrow cavity
6) characteristics of soft tissue tumor
7) relation with the adjacent anatomic structures
8) characteristics of malignancy.

Ad 1) – CT can accurately determine the topography of the tumor in the tissues where it develops: epiphysis, metaphysis, shaft of the bone and sometimes its relation to the growth cartilage. For soft tissue tumors: the muscle, group of muscles, the whole muscle or its fragment involved. The distance of the tumor from the articular spaces can be calculated, which is important in planning of conservative treatment.

Ad 2) – CT can assess the extent of bone lesions, the size of soft tissue tumors and the extent of the infiltration in the marrow cavity. These parameters are expressed in centimeters, according to the linear scale. The transverse, sagittal and longitudinal dimensions of the tumor are calculated. The tumor volume should also be calculated if it is possible with the CT program for calculation of irregular ellipsoid volume: the tumor volume is equal to sum of the volumes of the particular slices of 1.0 cm thickness. The slice volume is calculated automatically after delineation of the tumor contours in the slice, in the bone, soft tissue and marrow [36]. To assess the tumor volume, the solid volume formula, associated, however, with much higher measurement error, can also be used. We propose the simplified revolution ellipsoid volume formula: for lesions with a periosteal tumor $V = a \cdot b \cdot c \cdot 0{,}52$, for lesions limited to the bone $V = a \cdot b \cdot c \cdot 0{,}785$, where a, b, c correspond to three dimensions of the tumor: longitudinal, transverse and sagittal [37]. The baseline tumor volume is of prognostic significance; tumors with volume exceeding 100 ml are usually associated with worse prognosis, and changes in tumor size and volume as a result of chemotherapy are monitored to assess the tumor response to treatment [18, 38].

Ad 3) – bone destruction (osteolysis) and neoplastic osteogenesis with calcification (sclerotization) takes place in bone tumors. Both these proceses are visualized in CT images. Geographic type osteolysis with well-delineated clear borderlines is easier to assess. It is more difficult to differentiate between permeation osteolysis and "moth-eaten" pattern on the basis of CT – both types are visualized as small, unclearly delineated bone defects but both occur in malignant processes (fig. 1a, 6d).

Generally, CT assessment of osteolysis due to compression caused by a soft tissue tumor developing in the vicinity of a bone arouses no doubts. The contour of the bone is usually regular, without disruption of the periosteum. In cases of external infiltration of the bone by soft tissue tumors it is

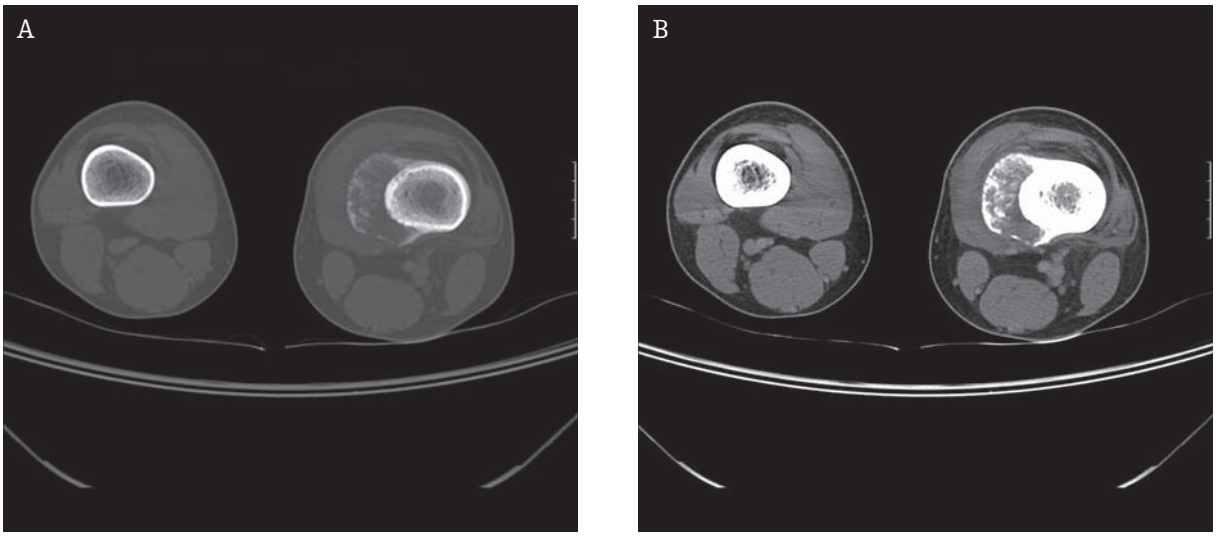

Figure 2. Osteogenic sa of the femur, preoperative CT (the same patient as in fig. 12). Sclerotic changes of cortical bone, calcification of periosteal reactions, calcifications in the extracortical tumor. Big regions of the tumor still uncalcified. **A**. Bone window. **B**. Soft tissue window.

sometimes difficult to determine unequivocally the direction of infiltration by CT. In massive osteolysis, the bone can be destroyed completely with bone fragmentation.

Sclerotization of the bone can be due to calcification of neoplastic osseous tissue or necrotic foci. Both these proceses are similarly presented by CT.

Ad 4) – normal periosteum is invisible in CT images, but all periosteal reactions, including thickening, can be visualized by CT. Computed tomography, because of its properties, is predestined to visualize such delicate structures as slightly calcified periosteum and its reactions. Images obtained in three planes yield complete information about all current periosteal reactions, giving a reliable visualization of their calcification (fig. 1a, 1b).

Ad 5) – bone marrow cavities of the long bones contain yellow bone marrow composed mainly of adipose tissue, which is characterized in CT by negative radiation attenuation coefficient values. Bone marrow with neoplastic infiltration changes its density, reaching positive values (fig. 1c) However, unequivocal differentiation between small infiltrations and edema of the bone marrow, possible in MRI, cannot be obtained with CT. Bone marrow cavity assessment is facilitated by comparative scans of both extremities, the normal and the tumor-affected one. It should be remembered that bone epiphyses (only of the radius and proximal femur in adults), the ribs, vertebrae, hip bones and sternum contain red bone marrow (involved in active hemopoiesis), which demonstrates positive radiation attenuation coefficient values.

Ad 6) – CT visualizes in a satisfactory way (although not perfectly as MRI) the character of soft tissue tumors, allowing to determine their structure (homogeneous, inhomogeneous). Differences in tissue density indicate the presence of solid and cystic parts, necrotization and necrotic areas, calcifications and ossifications. A significant increase of attenuation coefficient values within the tumor after contrast administration indicates pathologic vascularization, suggesting a malignant process. Soft tissue tumors can be regular or irregular, encapsulated or non-encapsulated, well or poorly delineated, with clear-cut or obscured borderlines. More invasive tumors are usually poorly delineated, partially encapsulated, or they have no capsule at all. Sometimes determination of their borderlines by CT is difficult; biphasic CT is usually helpful in such cases – a pathologically vascularized tumor shows more intensive contrast enhancement than the surrounding normal muscles. Tumors hypodense in comparison with muscle tissue, not enhanced with contrast medium, are also difficult to differentiate from the edematous area. Generally, edema accompanying the tumor shows lower attenuation coefficient values.

Similar analysis is carried out for soft tissue lesions accompanying bone tumors (fig. 1b, 6d)) In such cases, it is very important to delineate the tumor borders – whether it is subperiosteal, or extends beyond the periosteum, infiltrating the adjacent tissues.

Soft tissue lesions accompanying bone tumors may contain calcifications and ossifications (fig. 1a). Neoplastic osteogenesis is observed not only in osteosarcoma. In Ewing's sarcoma, calcifications are formed as a result of secondary mineralization of tumor necrosis foci. It is very difficult to determine the character of such calcifications. They are described in morphological terms, like in radiography, with respect to size – large, massive, small, fine; number – single, multiple; shape – patchy, cloud-like, granular, regular, irregular, character – merging, vague; degree of calcification – slightly calcified, calcified, significantly calcified. However, calcifications due to osteogenetic periosteal reaction – with lamellar or spicular structure are easy to distinguish.

Ad. 7) – CT generally allows to assess accurately the relation of tumor-related bone lesions to the growth cartilage and the articular structures; appropriately small slice thickness and low table shift rate, or reconstruction, should be applied. On overall assessment of the scan it can

be determined whether the soft tissue tumor is contained within one anatomic compartment, or extends beyond its limits (intra- or extra-compartmental tumors).

Ad 8) – CT, like X-ray and US, visualizes the characteristics of bone tumor malignancy. Thus, the type of the tumor – malignant or benign – can be determined in most cases. As indicated by our experience, it is superior to conventional radiography in this respect. The ultimate diagnosis, in case of both unequivocal and dubious imaging results, is established on the basis of histopathology.

Therapeutic period and preoperative examinations

CT is rarely used in bone tumors in the therapeutic period (see Methodology). If it is performed, tumor reactions to chemo- or radiotherapy are assessed according to the same criteria as in the preoperative examination, i.e.:
1) changes in tumor size and volume,
2) extent of necrosis, regression and viable tumor tissue areas,
3) changes in periosteal reaction.

The response to treatment is assessed – like in radiography, US and MRI – as:
– complete regression (CR),
– partial regression (PR),
– stabilization (SD),
– progression (PD).

Ad 1) In case of bone tumors, measurements of bone, marrow cavity and soft tissue lesions are mandatory, like in the diagnostic period. The preoperative examination must also determine accurately the distance of neoplastic lesions from the articular space – important for planning the procedure – mutilating or conservative. The tumor volume is calculated again, using the same method as in the diagnostic period. A decrease in tumor size does not indicate unequivocally good histological response to treatment and can be observed both in case of good and poor responses, whereas an increase usually indicates a poor response [6, 18, 38]. After induction chemotherapy of bone tumors, the paraosteal tumor usually decreases in size, whereas the extent of neoplastic process in the marrow cavity remains unchanged.

Ad 2) It is sometimes difficult to distinguish the necrosis, regression and viable tumor tissue areas in CT. If hyperdense, vascularized tissue is replaced by hypodense, non-contrast-enhanced areas, they can be regarded with high probability as necrotic areas. Regression and viable tumor tissue areas are practicably undistinguishable in CT. In the bone, remodeling of tumor lesions, i.e. calcification of neoplastic tissue and necrotic foci, known as sclerotization, is assessed (fig. 2a, 2b). Sometimes viable neoplastic osteogenesis can be misinterpreted as remodeling of neoplastic lesions or osteogenic periosteal reactions. Changes in isodense areas within the tumor, due to a decrease in size and formation of calcifications (fig. 2a, 2b), are also important from the point of view of response assessment. A decrease in their size is not a univocal indicator of response type, whereas an increase indicates poor response [6].

Ad 3) The assessment of periosteal reactions is very important to determine the response to treatment (fig. 2a). The changes in number and degree of calcification of lamellar reactions, repair reactions of the infiltrated periosteum, Codman's triangle remodeling and changes in spicular reactions - degree of calcification, incorporation and number of spicules are described [5, 13]. Generally reduced number of layers, complete repair of the periosteum disrupted at the site of the periosseous tumor and complete Codman's triangle remodeling indicate good response to the therapy [6]. Calcification and partial remodeling of periosteal reactions are observed both in good and in poor responses to tumor treatment [6].

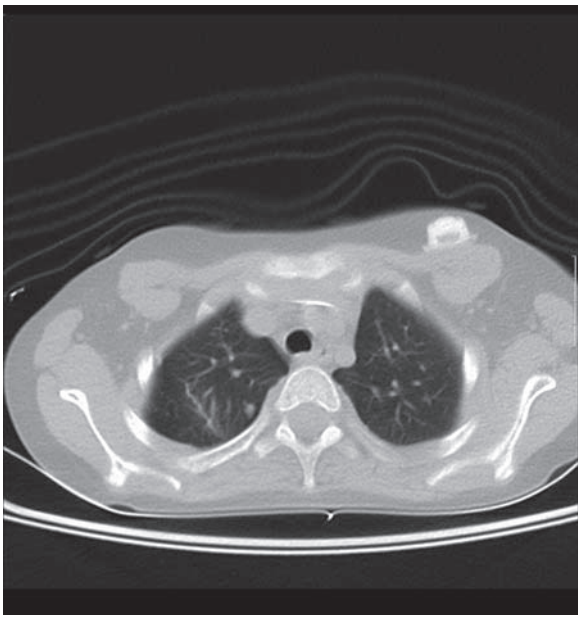

Figure 3. Follow-up study in a case of osteogenic sa. A pulmonary recurrence.

Chest CT in search of pulmonary metastases is first performed in the diagnostic period prior to the start of chemotherapy, and then in the preoperative period [1, 5, 25]. After the surgery, during adjuvant chemotherapy and after its completion, chest CT is performed according to the protocol applicable for a specific tumor and stage of the disease (localized or disseminated) – usually at 3-month intervals during the first 1-2 years, once in 6 months to 5 years [24]. There are no univocal criteria concerning further lung control, both with respect to the frequency of scans and to the follow-up period. Chest CT is usually performed once a year during the next 5-year period (fig. 3).

MAGNETIC RESONANCE IMAGING (MRI)

MRI is a particularly important method in the diagnostics of bone tumors. It is the optimal technique of bone tumor assessment, as it determines most accurately the extent of the neoplastic process in the bone, marrow cavity and soft tissue, as well as relation of the tumor to neurovascular structures [7, 25, 39].

The indications for MRI are as follows:
1. Verification of the diagnosis,
2. Determination of topography, size, morphology of the tumor and involvement of the bone marrow cavity,

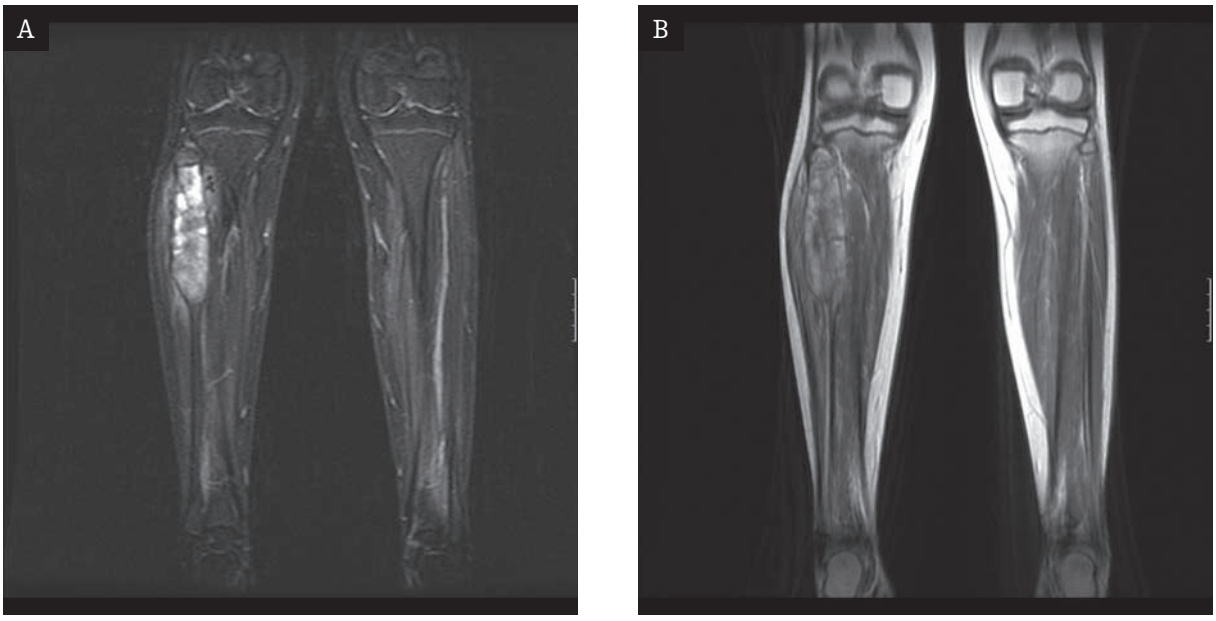

Figure 4. Ewing's sa of the fibula. MRI during initial chemotherapy, coronal plane. **A**. STIR. Inhomogenous tumor, infiltration of the medullary cavity does not exceed bony lesions. **B**. T1WI after Gd administration. Inhomogenous contrast enhancement of the tumor; calcifications and areas of regression do not enhance.

3. Monitoring of the therapy – assessment of response to chemotherapy, assessment of operability,
4. Diagnostics of local recurrence and metastases.

MRI has become indispensable in evaluation of tumor size, bone marrow cavity involvement and lesions of the adjacent soft tissues. It is a sensitive technique, but its specificity is inferior to sensitivity, it cannot also replace histopathology in assessment of malignancy of the lesion, although attempts of differentiation (benign / malignant) can be made in dynamic MRI after gadolinium administration, described below in the section concerning the assessment of chemotherapy effects. Differences in vascularization of these tumors are visualized in the rate and mode of increase of contrast enhancement, and, consequently, in the shape of the enhancement curve. The accuracy of assessment is improved after administration of a contrast medium which contains gadolinium. The subsequent scan allows to differentiate infiltration-related lesions from edematous areas surrounding the tumor. The possibility of obtaining images in all projections needed by the clinician (fig. 4, 5), without the necessity of secondary reconstruction from primary cross-section slices is important. The extent of the scan and the selection of an appropriate coil depend on the location and size of the tumor.

The limitation of the method is difficult differentiation of postoperative as well as post-chemo- and radiotherapy changes from residual lesions or relapses, however, dynamic MRI allows to overcome this problem. The presence of metallic postoperative elements and endoprostheses makes it more difficult, or sometimes impossible, to perform the scan [23, 40].

Apparatus

Imaging of musculoskeletal system tumors with equipment characterized by higher magnetic field intensity, optimally 1.5T, providing higher resolution, is recommended.

Methodology of MRI

Diagnostic period

Malignant bone tumors usually demonstrate high signal intensity in T2-weighted and low in T1-weighted images, have inhomogeneous structure and obscured borderlines [4]. The scan visualizes the extent of marrow cavity involvement, degree of cortical bone layer damage, size of the paraosteal tumor and signs of infiltration of adjacent tissues: the muscles and the neurovascular bundle. After contrast administration, inhomogeneous tumor enhancement is usually obtained, except for the necrotic and calcified areas (fig. 4b). In both sarcoma types, the presentation and involvement of the bone marrow is important for the therapeutic process, including the choice of method and extent of surgical treatment. MRI is the best method for assessment of changes within the bone marrow. It should be remembered that there are also physiological changes taking place in the marrow during development and maturation of the skeletal system, or due to marrow dysfunctions associated with the therapy or coincident diseases, e.g. anemia, when marrow reconversion may occur. Conversion of red to yellow bone marrow is gradual, asymmetrical and inhomogeneous. For tumor surgeons the extent of marrow cavity involvement determining the extent of the surgical procedure or irradiation field is the most important (fig. 4a, 5a). Accurate delineation of the pathology borderlines can reduce the number of secondary, more mutilating procedures, relapses or metastases [39].

The marrow is assessed simultaneously with the bone and paraosteal tumor changes. The examination include spin echo sequence in T1-weighted images (fig. 4b, 5b), T2-weighted images with fat saturation and STIR sequence (fig. 4a). The lesion extent is best assessed in T1-weighted images, which provide optimal contrast between red and

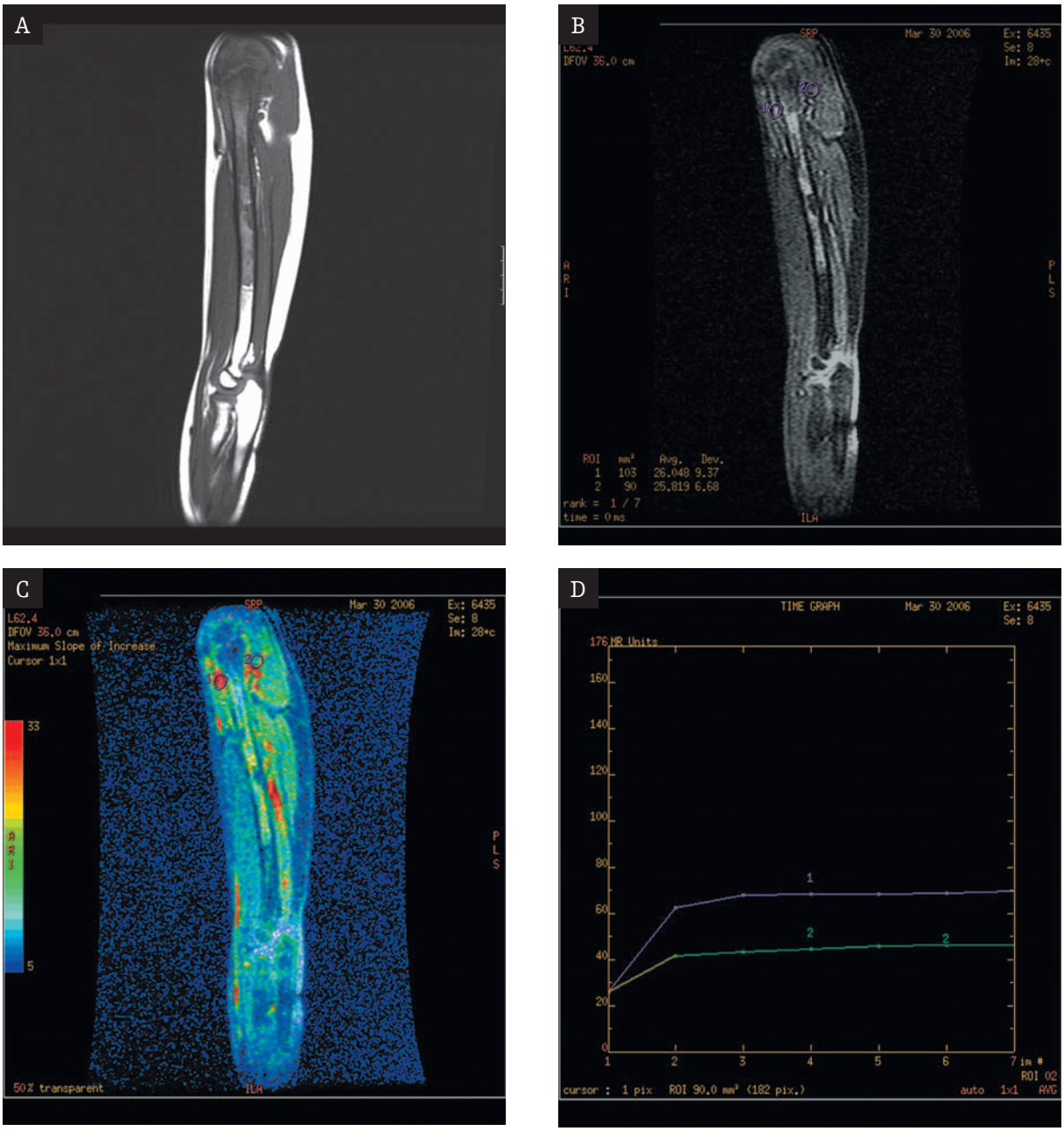

Figure 5. Ewing's sa of the humerus. MRI during initial chth, sagittal plane. **A**. T1WI. The extracortical tumor involves ½ of the bone, infiltation of the medullary cavity – 2/3. **B**. T1WI, FATSAT – part of dynamic examination. **C**. Color-coded contrast enhancement of the extracortical tumor on dynamic examination. **D**. The curve of contrast enhancement in a suspicious focus (1) is not typical of viable tumour tissue.

yellow marrow and pathologic changes, red marrow is hypointense in comparison with yellow one. T2-weighted images with fat saturation demonstrate high signal intensity both of the tumor and of necrotic, hemorrhagic or edematous areas. Therefore, the lesion size can be overestimated. Contrast administration in T1-weighted images with fat saturation allows to detect even small lesions of the bone marrow. In some cases, other sequences and quantitative methods are used in marrow assessment. Routinely, quick sequences allowing to reduce the time of the scan are used [39, 40]. Keeping in mind that the lesion extent in the marrow cavity can be larger than that of the bone and soft tissue tumor, the examination should be planned so that the visualized area includes all the affected marrow, and, optimally, the whole bone with both adjacent joints (fig. 5a).

Long scanning time requiring from the patient to remain motionless, can be a problem in children. For this reason, the most important sequences should be performed first. They include projection along the long bone axis (coronal or sagittal) in T1-weighted images, then the projection perpendicular to it (axial) in T2-weighted images with fat saturation, or STIR [4].

In any case, the relation of the tumor to vascular structures and nerves is indispensable. High tissue specificity

allows to differentiate the tumor and the surrounding edematous area from perivascular adipose tissue, whereas differentiation between tumor adherence or early infiltration of the neurovascular bundle is very difficult. However, involvement of neurovascular structures is very rare in osteosarcomas and accounts only for 4% of cases, so the above shortcoming is less important [4]. The possibility to perform angio-MRI sequence, both in the arterial and in the venous phase, is very useful for assessment of the relations between vascular structures and the tumor, their neoplastic infiltration and potential flow disturbances [40].

MRI performed in the diagnostic period involves the following measurements:
- length of bone marrow cavity involvement area,
- length of the paraosteal tumor in longitudinal section,
- two dimensions of the bone tumor and the paraosteal tumor in transverse section,

Therapeutic period and preoperative examinations – assessment of chemotherapy effects

Tumor response to induction chemotherapy is one of the most important information for clinicians in treatment of bone tumors. MRI allows the most reliable, non-invasive assessment, in which changes of tumor size, borderlines, signal intensity and contrast enhancement can be determined easily. It is necessary to assess tumor size to confirm the effects of the therapy and to plan the surgical procedure as conservative as possible [41]. However, tumor size alone does not provide sufficient information concerning response to treatment and does not correlate with histopathological response: e.g. an increase in size may indicate poor response, but may also result from a hemorrhage to necrotic area formed as a result of good response to chemotherapy [4, 23].

Signal intensity changes in osteosarcomas and Ewing's sarcomas also do not allow definite assessment of response to chemotherapy [4, 42]. Tumor regression is closely correlated with the duration of treatment and tumor biology (malignancy grade and sensitivity to chemotherapy). Response to treatment is demonstrated by a decrease of edema surrounding the tumor, presence of hemorrhagic foci, increase of necrotic areas and more intensive calcification of the tumor. Signal decrease in T2-weighted images after chemotherapy (cht) is a characteristic, but not very sensitive indicator of histopathologic response. It is a result of tumor tissue replacement by oligocellular matrix. Lower signal intensity is not univocal evidence of good response to treatment, confirmed histopathologically. Increased signal intensity can be due to edema, correlated with poor response to cht. On the other hand, high signal intensity in T2-weighted images can be also due to necrosis within the tumor or cyst-like post-hemorrhagic lesions, formed as a result of good histological response to chemotherapy. A low-signal margin on the tumor periphery, due to the presence of dense collagen fibers, is a characteristic feature in both sarcomas after cht.

Comparative assessment of T1-weighted images before and after intravenous contrast administration provides information about vascularization of the tumor. However, strongly enhanced residual lesions (or tumor recurrence) cannot be distinguished from granulation tissue newly formed as a result of the therapy, neovascularization of necrotic tissue or reactive congestion [4]. The tumor elements which are not enhanced by contrast include primarily the oligocellular tissues: fiber bundles, well-differentiated osteoid, cyst-like elements, chondromatous areas, ischemic necrosis, edema.

Dynamic examinations after contrast medium administration are definitely superior to static ones in this respect. In consecutive repetitions of the scan after intravenous administration of gadolinium, various parameters of contrast enhancement are determined: enhancement rate (index of contrast enhancement in time), time interval between the initial moment of enhancement in the blood vessel and in the tumor. Contrast enhancement curves are plotted on the basis of regions of interest selected by the examiner [42]. Assessment of the images after subtraction of images before and after contrast enhancement, which visualizes more clearly the enhanced areas, is also possible. Enhancement is assessed in the region of interest with reference to the signal obtained from unaffected muscles and blood vessels (fig. 5c, 5d). Rapid, early and high contrast saturation occurs in viable tumors accompanied by tissue edema [4, 42]. Three contrast enhancement curves have been described. Type I – rapid enhancement with subsequent plateau or signal decrease – is typical of a tumor. Type II – early enhancement increasing steadily – can occur both in malignant an in benign lesions. Type III – delayed, weak and slowly increasing enhancement – is typical of non-neoplastic lesions, such as necrosis and reactive changes after the therapy [44]. Rapid contrast enhancement observed in time to 6 s after arterial enhancement indicates the presence of viable tumor tissue. Slow rise of the enhancement curve in dynamic studies allows to exclude a malignant lesion [44]. The tumor tissue shows more intensive enhancement than the muscles, but weaker than the blood vessels. Necrotic areas demonstrate weaker enhancement than the muscles, but increasing slowly [43]. Edematous areas around the tumor show no contrast enhancement.

Monitoring saturation curve changes during chemotherapy helps to assess the response of the tumor to treatment. Marked reduction of enhancement and its increase rate after chemotherapy is regarded as a favorable effect. Good response to chemotherapy is characterized by at least 90% of necrosis within the tumor (grade III or IV in histopathological tumor necrosis assessment system according to Huvos) [21]. If no high-signal areas are present in first-pass MRI images, this suggests good response to cht. The accuracy of dynamic MRI in differentiation between good and poor response to cht is estimated to reach 85-100%. Therefore, the examination should be performed before and after neoadjuvant cht. High-signal areas present in first-pass images provide an indication for the pathologists, that these tumor areas feature active malignant process and require special, mapping-based assessment in the surgical material [44].

Dynamic MRI is also applicable in differentiation of post-therapy changes: postoperative, after radiotherapy, residual tumor tissue or tumor relapses. Dynamic studies also allow

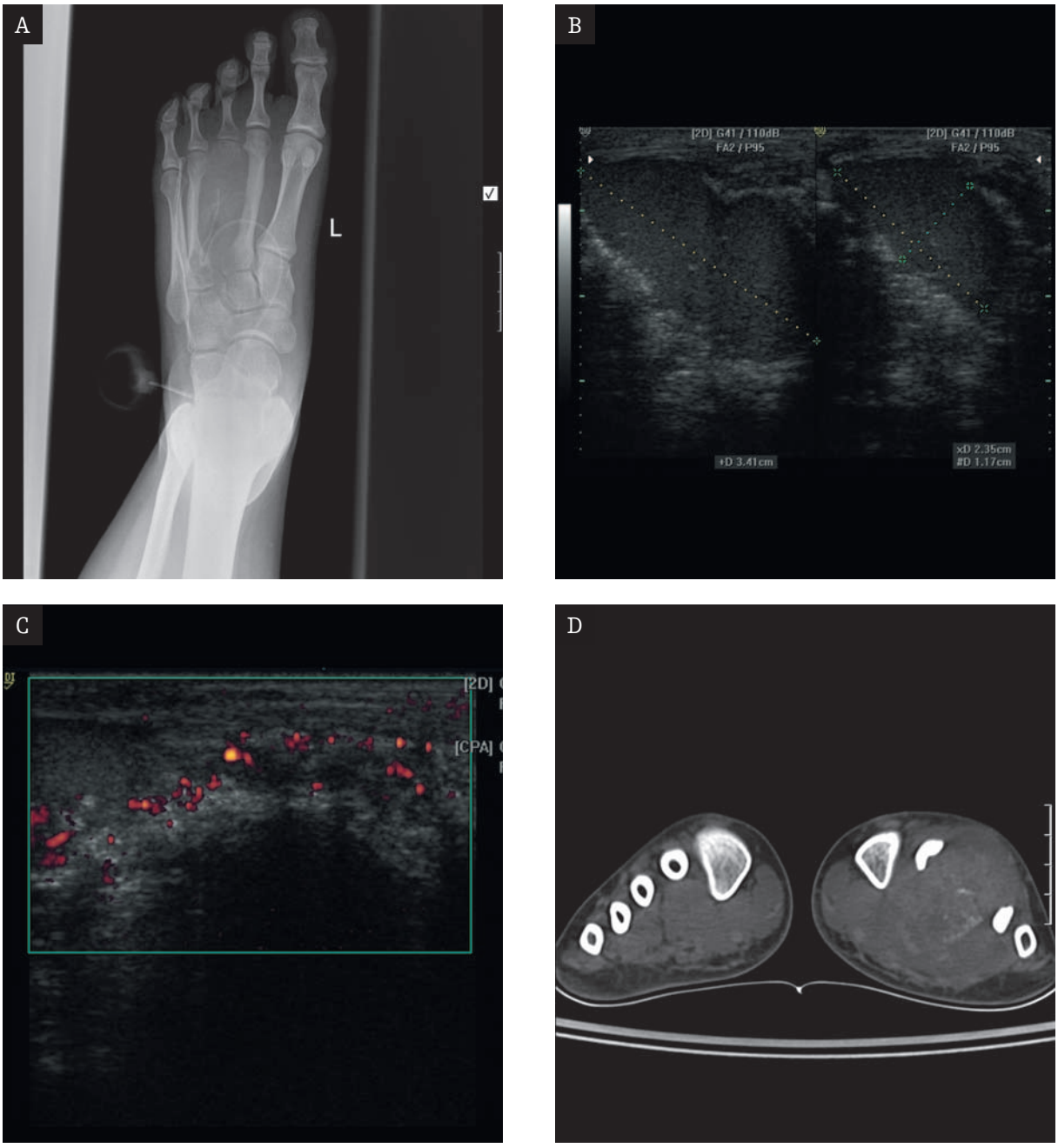

Figure 6. PNET of the 3rd metatarsal bone of the left foot. **A**. Plain film. Nearly total osteolysis. A big tumor after biopsy, drainage in the soft tissues. **B** and **C**. US. Homogenous, clearly demarcated mass in the diaphysis, bone destruction and calcification, pathological vessels among calcifications. **D**. CT. Nearly total osteolysis, a big, contrast-enhanced tumor in the soft tissues. Deformation and infiltration of the adjacent bones.

to distinguish a viable tumor from scarring, granulation tissue or inflammatory changes characterized by different enhancement curves.

Assessment of cht effects, as compared with histopathology, demonstrates ca. 70% accuracy in static MRI and ca. 85-90% accuracy in dynamic MRI [45].

In postoperative assessment of patients with limb prostheses, MRI is associated with considerable artifacts and less applicable for this reason. If there are no artifacts caused by the prosthesis (allograft after mutilating surgery), MRI can be applied in monitoring of patients for potential local recurrence and detection of residual tumor tissue after non-radical surgery. In such cases, T2-weighted images, STIR sequence and dynamic studies are predominantly used.

Magnetic resonance spectroscopy (MRS)

The usefulness of magnetic resonance spectroscopy in assessment of tumor response to chemotherapy is now being investigated. Phosphorus spectroscopy (31P MRS)

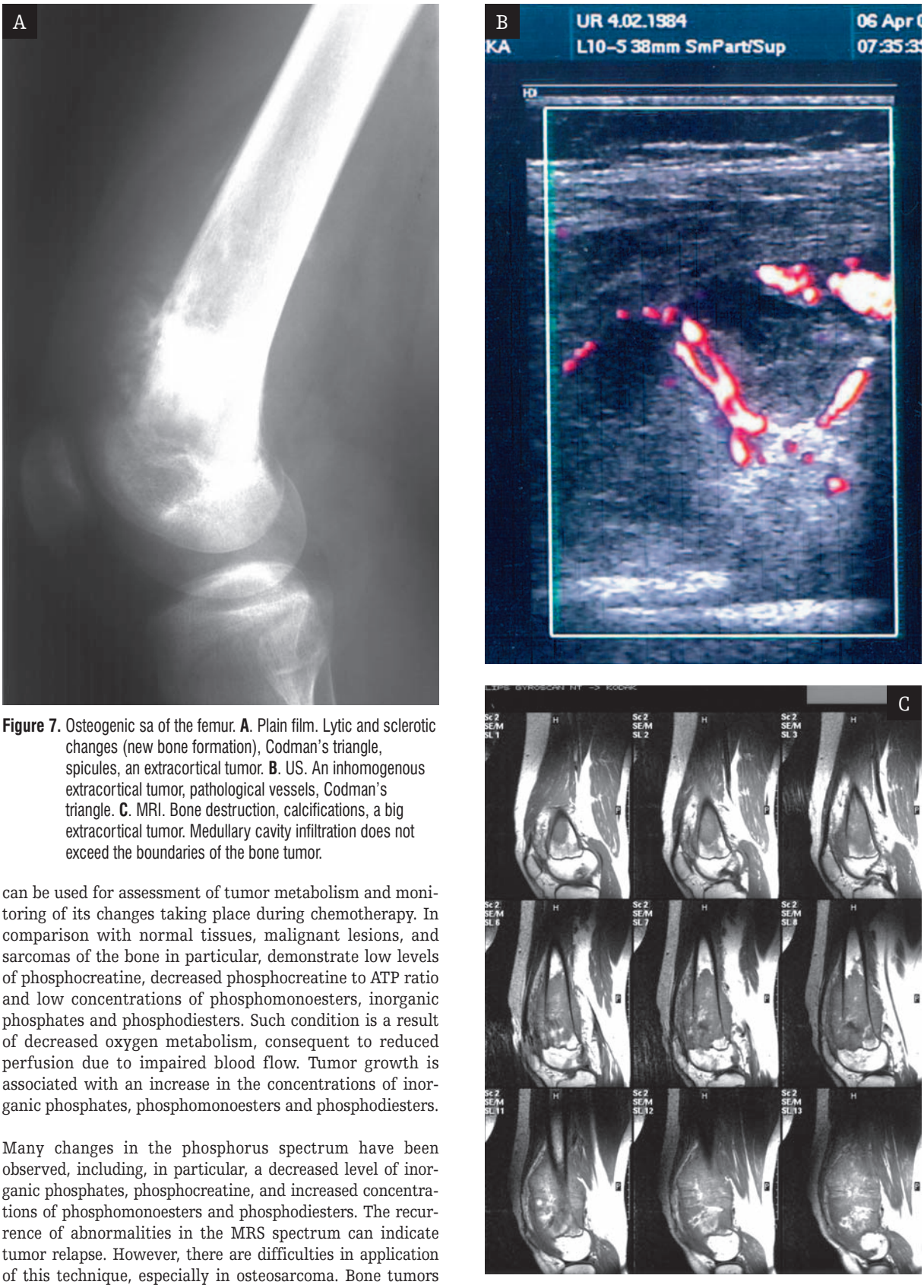

Figure 7. Osteogenic sa of the femur. **A**. Plain film. Lytic and sclerotic changes (new bone formation), Codman's triangle, spicules, an extracortical tumor. **B**. US. An inhomogenous extracortical tumor, pathological vessels, Codman's triangle. **C**. MRI. Bone destruction, calcifications, a big extracortical tumor. Medullary cavity infiltration does not exceed the boundaries of the bone tumor.

can be used for assessment of tumor metabolism and monitoring of its changes taking place during chemotherapy. In comparison with normal tissues, malignant lesions, and sarcomas of the bone in particular, demonstrate low levels of phosphocreatine, decreased phosphocreatine to ATP ratio and low concentrations of phosphomonoesters, inorganic phosphates and phosphodiesters. Such condition is a result of decreased oxygen metabolism, consequent to reduced perfusion due to impaired blood flow. Tumor growth is associated with an increase in the concentrations of inorganic phosphates, phosphomonoesters and phosphodiesters.

Many changes in the phosphorus spectrum have been observed, including, in particular, a decreased level of inorganic phosphates, phosphocreatine, and increased concentrations of phosphomonoesters and phosphodiesters. The recurrence of abnormalities in the MRS spectrum can indicate tumor relapse. However, there are difficulties in application of this technique, especially in osteosarcoma. Bone tumors are heterogeneous and the indication of voxel localization is not standard. However, it seems that hopes for the future can be associated with this noninvasive "chemical biopsy" [23].

Recently published reports describe the use of proton spectroscopy (1H MRS) in differentiation of changes in bone and soft tissue tumors. Spectroscopy using the single voxel

technique with multi-echo sequence and setting the voxel in strongly enhanced areas in first-pass images in dynamic MRI demonstrates the choline peak in malignant lesions and on this basis malignant and benign lesions can be differentiated with 95% sensitivity, 82% specificity and 89% accuracy [46].

Conclusion

Long-term experience of our Department in the diagnostics of osteogenic sarcoma and Ewing's sarcoma at all stages of the disease has provided the basis for the proposed diagnostic algorithm, applicable in case of these tumors.

I. Diagnostic period

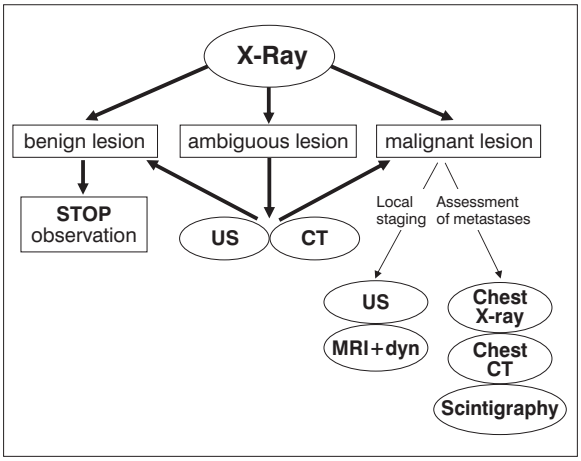

II. During induction chemotherapy
X-ray
US
also chest CT (in case of metastases)

III. Preoperative period (after induction cht)
X-ray with measurement
MRI+dyn
US
Chest CT
CT of the lesion if necessary

IV. Follow-up after the therapy
X-ray
US
Chest CT
also MRI if a relapse is suspected

Diagnostic efficiency of imaging modalities in case of osteogenic sarcoma and Ewing's sarcoma:

Diagnostic field	X-ray	US	CT	MRI
Bone structure	+	-	++	-
Periosteum	+	+	++	+/-
Marrow cavity	-	-	+	++
Soft tissue	-/+	+	+	++

Examples of imaging diagnostics in Ewing's sarcoma/PNET are illustrated in figs. 6a-d, and in osteogenic sarcoma – in figs. 7a-c.

References:

1. Woźniak W: Leczenie dzieci z najczęstszymi nowotworami kości, mięsak kościopochodny (Treatment of children with most common bone tumors, osteogenic sarcoma – in Polish). Monog., IMiD (Institute of Mother and Child), Warsaw 1998; 8–30.
2. Bodner G, Schocke MFH, Rachbauer FI et al.: Differentiation of Malignant and Benign Mosculoskeletal Tumors: Combined Color and Power Doppler US and Spectral Wave Analysis, Radiology 2002, 223: 410–416.
3. Liebhart M: Problemy diagnostyki histopatologicznej guzów kości okresu dziecięco-młodzieżowego (Problems with histopathological diagnostics of bone tumors of childhood and adolescence period – in Polish). In: Stoba Cz, Czauderna P (eds.): Guzy kości u dzieci, diagnostyka i leczenie (Bone tumors in children, diagnostics and treatment – in Polish). Wydawnictwo Folium, Lublin 1997; 35–39,
4. Davies MA: Imaging in skeletal paediatric oncology. Eur J Radiol 2001, 37: 79–94.
5. Wittig JC, Bickels J, Priebat D et al.: Am Fam Physician 2002; 65: 1123–32, 1135–6.
6. Kopyś-Wiszniewska I: Obrazy okostnej w tomografii komputerowej w złośliwych guzach kości przed i po chemioterapii (Periosteal computed tomography images in malignant bone tumors before and after chemotherapy – in Polish). Dissertation for Ph.D. degree. Institute of Mother and Child, Warsaw, 2000.
7. Hide II G: Osteosarcoma, Classic http:/www.emedicine.com/radio/topic504.htm (accesed 4.11.2005).
8. Lopez JI: Usefulness and limitations of ultrasound-guided core biopsy in the diagnosis of musculoskeletal tumors. APMIS 2005; 113: 353–60.
9. Talbot JN, Kerron K, Gutman FI et al. GDF-PET in localization of cancers of unkown primary arigin. Presse Med 2006; 35 (9Pt2): 1371–1376.
10. Goodlin GS, Shulkin BL, Kaufman RA et al.: PET/CT characterization of fibroosseus defect in children: 18F-FDG uptake can mimic metastatic disease. Am J Roentgenol 2006; 187(4): 1124–1128.
11. Mentzel HJ, Kebtouche K, Sauer D et al.: Comparison of Whole-body STIR–MRI and 99mTc-methylene-diphosphonate scintigraphy in children with suspected multifocal bone lesions. Eur Radiol 2004; 14(12): 2297–2302.
12. TateiskiV, Yamaguchi V, Maeda T et al.: Staging performance of carbon-11 choline positron emission tomography/computed tomography in patients with bone and soft tissue sarcoma: comparison with conventional imaging. Cancer Sci 2006; 97 (10): 1125–1128.
13. Buraczewski J, Dziukowa J: Radiodiagnostyka zmian nowotworowych i nowotworopodobnych kości i tkanek miękkich (Radiodiagnostics of bone and soft tissue tumors and tumor-like lesions – in Polish). W: Leszczyński S (ed.): Radiologia. PZWL Warsaw, 1993, T. III: 215–320.
14. Tacikowska M: Symptomatologia radiologiczna mięsaka Ewinga (Radiological symptomatology of Ewing sarcoma – in Polish). Dissertation for Ph.D. degree. Oncology Center Institute, Warsaw, 1997.
15. Chindia ML, Guthua SW, Awangge DO et al.: Osteosarcoma of the maxillofacial bones in Kenyans. J Craniomaxillofac Sur, 1998; 26(2): 98–101.
16. Mandahl N: Genetyka nowotworów kości. (Genetics of bone tumors – in Polish). In: Stoba Cz, Czauderna P (eds.): Guzy kości u dzieci, diagnostyka i leczenie (Bone tumors in children, diagnostics and treatment – in Polish). Wydawnictwo Folium Lublin, 1997; 41–46.
17. Woźniak W: Nowotwory Kości (Bone tumors – in Polish). In: Bożek J (ed.): Nowotwory wieku dziecięcego (Childhood tumors). PZWL Warsaw 1989; 92–103.
18. Pochanugool L, Subhadharaphandou T, Danachai M et al.: Prognostic factors among 130 patients with osteosarcoma. Clin Orthop 1997; 345: 206–214.
19. Feydy A, Bui M, Guerini H et al.: Imaging features of parosteal osteosarcoma. http://rsna 2005.rsna org/rsna 2005/v2005/conference/event_ display.cfm?id=666018em_id=4414870.

20. Romaniuk-Doroszewska A: Obraz rentgenowski typów histopatologicznych sarcoma osteogenes przed i po chemioterapii (Radiography images of histopathologic types of sarcoma osteogenes before and after chemotherapy – in Polish). Dissertation for Ph.D. degree. Institute of Mother and Child, Warsaw, 1999.
21. Wunder JS, Paulian G, Huvos AG et al.: The pathological response to chemotherapy as a predictor of the oncological outcome of operative treatment of Ewing sarcoma. J Bone Joint Surg Am 1998; 80: 1020–1033.
22. Winnicki S, Romaniuk-Doroszewska A: Znaczenie konwencjonalnej diagnostyki rentgenowskiej u dzieci z sarcoma osteogenes i sarcoma Ewingi. Spostrzeżenia własne. (Value of conventional radiographic diagnostics in children with sarcoma osteogenes and sarcoma Ewingi. Own observations – in Polish). Medycyna Wieku Rozwojowego 1997; L3: 439–447.
23. Van der Woude H-J, Bloem JL, Hogendoorn PCW: Preoperative evaluation and monitoring chemotherapy in patients with high-grade osteogenic sarcoma and Ewing's sarcoma: review of current imaging modalities. Skeletal Radiology 1998; 27: 57–71.
24. Bearcroft PW, Davies AM: Follow-up of musculoskeletal tumors 2. Metastatic disease. Eur Radiol 1999; 9: 192–200.
25. Ilaslan H, Sundaram M: Advances in Musculoskeletal Tumor Imaging. Orthop Clin N Am 2006; 37: 375–391.
26. Wermeński K, Brągoszewska H: Obraz ultrasonograficzny patologicznego unaczynienia tkanek miękkich w prezentacji 3D. Doniesienie wstępne (Ultrasound imaging of pathologic soft tissue vascularization in 3D presentation. A preliminary report – in Polish). Ultrasonografia 2001; 5: 11–14.
27. Wermeński K, Brągoszewska H: Obraz ultrasonograficzny patologicznego unaczynienia tkanek miękkich po wzmocnieniu kontrastowym za pomocą preparatu Levovist (Schering). Doniesienie wstępne (Ultrasound imaging of pathologic soft tissue vascularization after contrast enhancement with Levovist (Schering). A preliminary report – in Polish). Ultrasonografia 2001; 5: 7–10.
28. Krzanowski M, Plichta A: Atlas ultrasonografii naczyń (Atlas of vascular ultrasound – in Polish), Medycyna Praktyczna, Kraków 2000; 39–48: 270–278.
29. Szopiński K: Ultrasonograficzne środki kontrastowe (Contrast media used in ultrasound scanning – in Polish). In: Malek G (ed.): Ultrasonografia Dopplerowska, zastosowanie kliniczne (Doppler ultrasound, clinical applications). Medipage 2003, 175–182.
30. Hofer M: Basic physical and technical principles. W: Teaching Manual of Color Duplex Sonography. A workbook on color duplex ultrasound and echocardiography. Fronek A. (ed.). Thieme 2004, 7–16.
31. Kellner H, Reimers CD: Zasady wykonywania ultrasonograficznego badania narządów ruchu (Principles of ultrasound scanning of the locomotor organs – in Polish). In: Kellner H, Reimers CD: Ultrasonografia układu ruchu (Ultrasonography of the locomotor system). Urban & Partner, Wrocław 1998, 12–14.
32. Bramer MA, Gubler MF Maas M et al.: Colour Doppler ultrasound predicts chemotherapy response, but not survival in paediatric osteosarcoma. Pediatr. Radiol. 2004; 34: 614–619.
33. Walecki J, Ziemiański A: Rezonans magnetyczny i tomografia komputerowa w praktyce klinicznej (Magnetic resonance and computed tomography in clinical practice – in Polish). Springer PWN, Warsaw 1997, 297–299.
34. Petterson H et al.: The encyclopaedia of medical imaging. The NICER Institute, 1999; t. I.
35. Tacikowska M: Propozycje standaryzacji badań TK w guzach kości (Proposals for standardization of CT examinations in bone tumors – in Polish). Pol Przegl Radiol, 1997; 62: 251.
36. Wermeński K: Pomiar objętości guza za pomocą badania TK (Measurement of tumor volume by CT – in Polish). In: Woźniak W: (Treatment of children with most common bone tumors, osteogenic sarcoma). Monog., Institute of Mother and Child, Warsaw 1998; 32–33.
37. Draft AW, Jurgens H.: Diagnostic and pre-therapy evaluation. EICESS 92. MedRes Counsil 1993; 5: 22.
38. Shin KH, Suh JS et al.: Tumor volume change as predictor of chemotherapeutic response in osteosarcoma. Clin Orthop and Rel Res. 2000; 376: 200–208.
39. Vande Berg BC, Malghem J, Lecouvet FE et al.: Classification and detection of bone marrow lesions with magnetic resonance imaging, Skeletal Radiology, 1998, 27: 529–545.
40. Stajgis M: Szpik kostny w obrazie MR (Bone marrow in MR imaging – in Polish). [In:] Walecki J, Ziemiański A (eds.): Rezonans magnetyczny i tomografia komputerowa w praktyce klinicznej (Magnetic resonance and computed tomography in clinical practice). Springer PWN, Warsaw 1997, 312–325.
41. Saifuddin A: The accuracy of imaging in the local staging of appendicular osteosarcoma Skeletal Radiol2002, 31: 191–201.
42. Bloem JL, van der Woude HJ, Geirnaerdt M et al.: Does magnetic resonance imaging make a difference for patients with musculoskeletal sarcoma? Brit J Radiol 1997, 70: 327–337.
43. Dyke JP, Panicek DM, Healer JH et al.: Osteogenic and Ewing Sarcomas: Estimation of Necrotic Fraction during Induction Chemotherapy with Dynamic Contrast-enhanced MR Imaging. Radiology 2003, 228: 271–278.
44. Verstraete K, Lang P: Bone and soft tissue tumors: the role of contrast agents for MR imaging. Eur J Radiol 2000, 34: 229–246.
45. Brisse H, Ollivier L, Edeline V et al.: Imaging of malignant tumours of long bones in children: monitoring response to neoadjuvant chemotherapy and preoperative assessment. Pediatr Radiol 2004, 34(8): 55595–605.
46. Chien-Kuo W, Chun-Wei L, Tsyh-Iyi H et al.: Characterisation of Bone and Soft-Tissue Tumors with In Vivo 1H MR Spectroscopy: Initial Results. Radiology 2004; 232: 599–605.